Journal of Solid State Chemistry **142,** 100–107 (1999)
Article ID jssc.1998.7993, available online at http://www.idealibrary.com on IDEAL®

Preparation and Characterization of Niobium Carbide and Carbonitride

Hak Soo Kim,* Guy Bugli, and Gérald Djéga-Mariadassou[1]

*Université P. & M. Curie, Laboratoire Réactivité de Surface, CNRS URA 1106, Casier 178, 4 Place Jussieu, 75252 Paris Cedex 05, France; and *Division of Chemical Engineering, Sun Moon University, 100 Kalsanri Tangjeongmyeon, Asansi, Chung Nam, Korea*

Received April 21, 1998; in revised form July 16, 1998; accepted July 24, 1998

Unsupported niobium carbide powders of NbC were prepared by carburization of commercial niobium pentoxide in flowing CH_4–H_2 mixtures. Several routes of synthesis were investigated, leading to final carbides with specific surface areas ranging from 10 to 50 $m^2 g^{-1}$. During direct carburization, after the first step of reduction of Nb_2O_5 to NbO_2, a long induction period which was succeeded by an acceleratory period, was observed for the reduction/carburization to NbC. In the presence of a catalyst of methane decomposition, this induction period was eliminated but the superficial carbon free contamination of the final carbide was increased. However, this contamination can be removed by a reducing treatment and CO chemisorption can be observed. The preparations through niobium oxynitride lead to face-centered cubic carbonitrides with specific surface areas ranging from 27 to 49 $m^2 g^{-1}$. Chemical composition and cell parameter of these cabonitrides vary slightly with the synthesis conditions. After a reducing treatment, as for NbC, CO chemisorption was also observed.

INTRODUCTION

Although there is some controversy about the relationships between the phases in the niobium–carbon system (1, 2), there are basically at least three well-characterized solid carbide phases:

(i) A solid solution which keeps the body-centered cubic lattice of the metal and which can dissolve up to 6 at.% of carbon at about 2608 K, the eutectic temperature (3–6), the lattice parameter increasing with the carbon content.

(ii) A hemicarbide Nb_2C which has a very narrow range of homogeneity at room temperature. The high temperature γ-Nb_2C phase presents a hexagonal structure (disordered L′3 type) (3–6). At a lower temperature or in presence of impurities such as oxygen (7) another crystal structure can occur by ordering of carbon atoms. Among the possible ordered structures, the hexagonal β-Nb_2C (ordered ε-Fe_2N type) and the orthorhombic α-Nb_2C phase similar to ξ-Fe_2N type have been found (8–11).

(iii) A monocarbide NbC_x, which is an homogeneous phase from approximatively $NbC_{0.7}$ to NbC. The high temperature NbC_x phase, also designated by δ-NbC (4, 5), shows a random face-centered cubic structure whose lattice parameter increases from 4.412 to 4.470 Å with carbon content (12–14). As with hemicarbide, ordered structures could exist (15) such as δ'-Nb_6C_5 (16–21).

Niobium carbides can be synthetized by a variety of methods including direct union of the elements at high temperature (22, 23) or by self-propagating high-temperature reaction (24, 25), carburization of the oxides by carbon (26–29) or methane–hydrogen mixtures (30–32), carburization of niobium pentahalide (33–38). Generally, these syntheses occur at high temperature and lead to materials of low surface area which limit their use in catalysis. However, some preparations of ultrafine powders of niobium carbides by spray-dried-powder technique (36) or by mechanochemical synthesis (39, 40) or by plasmachemical process (37, 38) have been reported. More recently, niobium carbide with a high specific surface area has been obtained by temperature-programmed reaction between niobium aerogel oxide and a mixture of methane and hydrogen (41, 42).

Previous work (41) has pointed out that the carburization of niobium pentoxide to niobium monocarbide could be carried out at 1173 K by flowing a CH_4–H_2 gas mixture. They have found the method to be successful and it did not show any induction period. Controversely, depending on the origin and preparation mode of Nb_2O_5, some very low initial carburization rates were observed during the present work, leading to a very long induction time for the reaction to proceed. One of the aims of the present paper was to report the main features of the carburization process of such a niobium oxide precursor presenting a long induction period before carburizing. Different ways to avoid this problem were studied. Several routes of synthesis for carburizing commercial niobium pentoxide were therefore investigated using a methane–hydrogen mixture at low temperature in

[1] To whom correspondence should be addressed. E-mail: djega@ccr.jussieu.fr.

0022-4596/99 $30.00

order to also avoid carbon contamination and sintering if possible and, hence, to obtain final products with suitable surface areas for catalytic purposes. These routes, adapted from these used successfully for molybdenum carbide synthesis (42–45), are direct carburization, carburization in the presence of catalyst of methane decomposition, and carburization through an oxynitride of high surface area. The synthesized carbides are characterized by physical and chemical methods.

EXPERIMENTAL

The niobium pentoxide (99.9%, Prolabo) and commercial $NiMo/Al_2O_3$ catalyst (Institut Français du Pétrole) were used as received. Prolabo niobium pentoxide is a mixture of two modifications (monoclinic M–Nb_2O_5 and orthorhombic T–Nb_2O_5) with 15 wt% of T-phase (46). Nickel (or rhodium)-niobium pentoxide precursors were prepared by the incipient wetness method: after impregnation of pentoxide with an appropriate volume of aqueous solution of nickel (or rhodium) chloride, the impregnated samples were dried at 393 K for 1 h in air and then linearly heated up to 993 K and maintained at this temperature for 1 h. Gases from Air Liquide were used without further purification: CH_4 (custom grade, 99.95%), O_2 (custom grade, 99.95%), He (high purity grade, 99.995%) and H_2 (high purity grade, 99.995%). Gaseous mixtures were prepared using mass flowmeters (Brooks 8530 Tr).

The synthesis of carbides was performed in a tubular quartz reactor provided with a coarse quartz fritted disk for holding the solid starting oxide. In addition, two stopcocks could isolate this reactor, avoiding, if necessary, any contact of the sample with air during its transfer toward an another device. The reactor was heated by an electric furnace, whose temperature was monitored with a programmable linear rate temperature controller (Setaram TGC 85). The gaseous products evolved during the carburization were analyzed with a gas phase chromatograph equipped with an automatic injection valve and a thermal conductivity detector linked to a peak integrator (Hewlett Packard 3390A). A 1.8-m long, 3-mm diameter Porapak N or Carbosieve S-II column was used for the separation of gases. Before exposure to air, each sample was passivated at room temperature, in a flowing mixture of 1 vol.% O_2 in He, to prevent a further rapid bulk oxidation.

Specific surface areas S_g of carbides were determined by physisorption of N_2 at 77.3 K using a Quantasorb Jr. dynamic sorption system linked to a catharometer detector. The relative pressures generally applied were in the range of 0.1 to 0.3. The specific surface areas were calculated using the BET method (47), with a 0.162 nm^2 section area for the adsorbed N_2. Corresponding particle sizes, assuming a spherical shape, were calculated from the equation $Dp = 6/S_g . \rho$ where ρ is the density of solid.

Irreversible CO chemisorption was carried out at room temperature by a pulsed method. This method consisted of the injection of a known quantity of CO, using an automatic valve, in a flowing helium carrier which passed through the carbide sample. After each injection, the quantity of CO not chemisorbed was measured using a conventional catharometric device.

A Siemens D500 automatic diffractometer was used for the XRD powder patterns of the various solid phases. The $K\alpha$ wavelength of copper was selected by a graphite diffracted beam monochromator. All data were collected on an IBM computer and analyzed with the SOCABIM diffrac-AT software. The identification of the different phases was made using the JCPDS library for M-Nb_2O_5 (No. 30-872), T–Nb_2O_5 (No. 30-873), NbO_2 (No. 34-898), NbC (No. 38-1364). The lattice parameter of the face-centered cubic niobium carbide was determined using a refinement program (48). The average size D_c of coherently diffracting domains perpendicular to (*hkl*) planes was evaluated by the Scherrer formula (49) from the half-width of the (*hkl*) X-ray diffraction line corrected for instrumental broadening.

Thermogravimetric analysis (TGA) was performed using a Seteram MTB 10-8 microbalance equipped with an electric furnace and its programmable temperature controller (Seteram RT3000). The sample weight and temperature were recorded continuously with a Meci two-pen recorder. The microbalance was connected to a vacuum system composed of a turbomolecular pump (Leybold Turbovac 50) backed by a Trivac pump, which could achieve a dynamic vacuum of about 10^{-4} mbar.

The elemental analysis was performed either by the Service Central d'Analyses du CNRS (Vernaison) or by the UPMC Laboratory for Chemical Analysis.

RESULTS

Direct Carburization of Nb_2O_5

The carburization of niobium pentoxide was first attempted in a tubular quartz reactor using a heating rate of 2.5 K min^{-1} from 298 to 1123 K in a 10% (v/v) CH_4/H_2 mixture flowing at a molar space velocity of 360 h^{-1}. The final temperature of 1123 K was maintained for 3 h. The gas composition during the preparation was monitored by gas phase chromatography (GPC). No carbon oxide formation nor methane consumption were detected, only water formation was observed. The water formation profile consisted of a broad peak with a small shoulder at 1053 K and a maximum at 1123 K when the temperature reached its maximal and ending value (Fig 1). In a separate experiment, the synthesis was also followed by thermogravimetry in a static atmosphere of 10% (v/v) CH_4/H_2 mixture. A P_4O_{10} trap was installed inside the microbalance to absorb the water vapor produced during the synthesis.

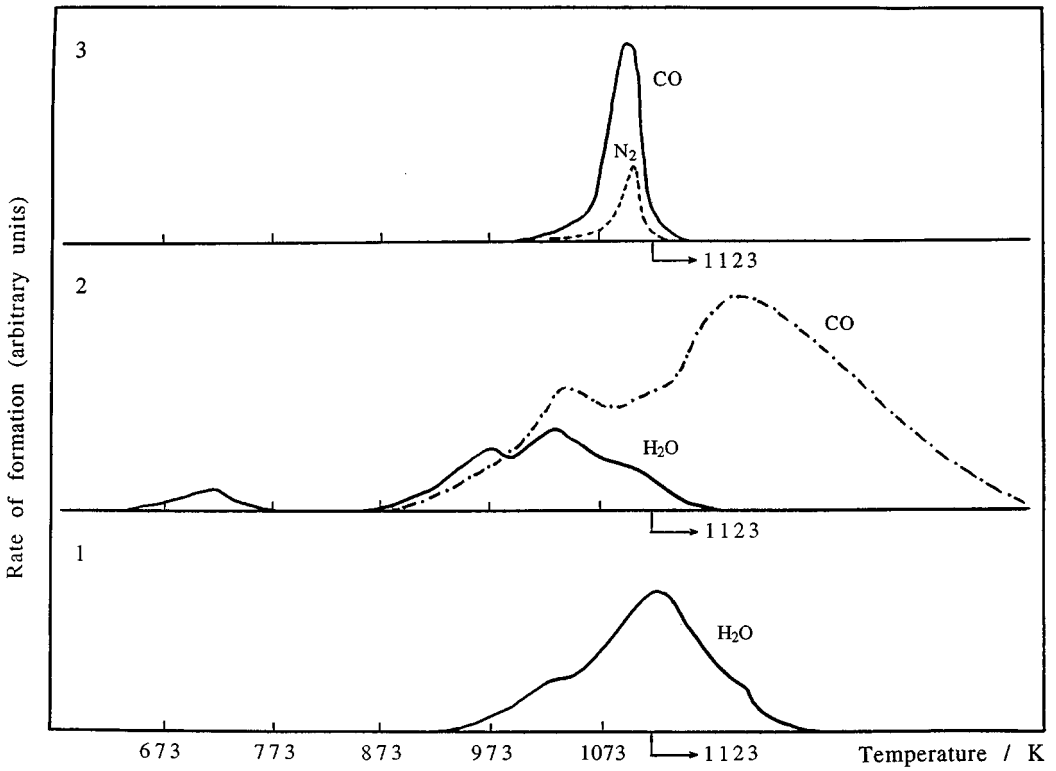

FIG. 1. Gas formation profiles during the reduction/carburization process of (1) Nb_2O_5, (2) 1 wt.% Ni/Nb_2O_5 mixture, and (3) niobium oxynitride NbN_xO_y, using a 10% (v/v) CH_4/H_2 mixture flowing at a molar space velocity of 360 h^{-1} with a heating rate of 2.5 K/min.

The TGA curve is displayed in Fig. 2. When the preparation was halted at about 20% of the Nb_2O_5 reduction to NbO_2 (point "a" in Fig. 2), which corresponds to the shoulder in the water formation profile (Fig. 1), it was found by XRD that the T–Nb_2O_5 phase had disappeared, the sample being a mixture of M-Nb_2O_5 and NbO_2. After 6 h at 1123 K (point "b" in Fig. 2), in agreement with the weight loss of the sample, XRD showed the presence of only NbO_2. However, if TGA was continued over a longer period of time, it evidenced, after an induction period of 2 or 3 h, a very slow but accelerated weight loss. After 33 h at 1123 K, 35% of niobium oxide was carburized to δ-NbC_x. The x stoichiometry of δ-carbide phase was evaluated by XRD, using the lattice parameter–carbon content relation, determined by Kempter *et al.* (14). In view of these results, the carburization of Nb_2O_5 in a tubular quartz reactor was reinvestigated, modifying several operating conditions such as the final temperature of carburization, the duration of isothermal treatment, or the concentration of methane. Generally, after the reduction stage of Nb_2O_5 to NbO_2, variable induction periods from 5 to 17 h, depending on temperature and concentration of methane, were observed before isothermal reduction carburization itself. Then, a long acceleratory period took place up to about 40–60% of the extent of the reaction. During the carburization process the consumption of methane followed the formation of carbon monoxide and no formation of water was detected. The final weight loss was very close to the theoretical weight loss of 21.06% expected for the formation of NbC. This result is consistent with that of the chemical analysis and points out the low contamination by free carbon. The characteristics of the final products are summarized in Table 1.

Carburization of Nb_2O_5 in the Presence of Metal Catalyst

Carburization of niobium pentoxide impregnated with nickel (or rhodium) metal, denoted by Ni(or Rh)/Nb_2O_5, was studied in the same manner as that used for the carburization of the pure pentoxide. Figures 1 and 2 display, respectively, the results of gas chromatography and thermogravimetry analysis for Ni/Nb_2O_5 mixture with 1 wt% of metal. The rate of water formation passes through three maxima at 723, 978, and 1038 K. The first peak was due to the reduction of nickel oxide, the two others were due to the reduction of pentoxide to dioxide. The carbon monoxide formation profile was composed of a small peak with a maximum at 1053 K and a broad peak with a maximum in the isothermal region. The consumption of methane was simultaneous with carbon monoxide formation except at the end

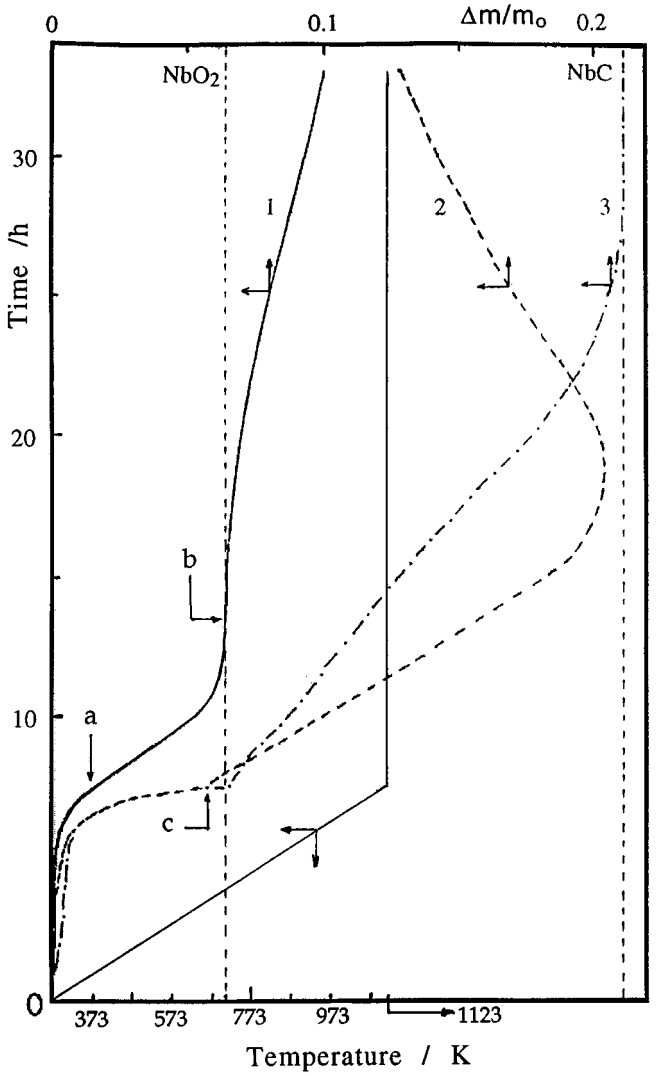

FIG. 2. Thermogravimetric curves during the reduction/carburization process of (1) Nb_2O_5, (2) 1 wt.% Ni/Nb_2O_5 mixture, and (3) 1 wt.% Rh/Nb_2O_5 mixture in a static atmosphere of 10% (v/v) CH_4/H_2 mixture with a heating rate of 1.75 K/min. The vertical dotted lines indicate the location of theoretical weight plateau corresponding, respectively, to the NbO_2 and NbC formation.

of the synthesis, where a weak methane consumption remained due to methane decomposition. This is evidenced on the TGA curve (Fig. 2, 2) by the final increase in the weight of the sample, due to the carbon deposition resulting from methane dissociation. When the preparation was halted at point "c" (Fig. 2), XRD showed the presence of the NbO_2 phase only. The diffraction pattern of the passivated final product was very close to those of δ-NbC (Fig. 3). As previously, the stoichiometry x of NbC_x obtained was determined using its lattice parameter value.

Gas formation or consumption profiles and thermogravimetric curve during the carburization of Rh/Nb_2O_5 precursor present features very similar to those of Ni/Nb_2O_5. However, it was observed that the rhodium oxide was reduced at a lower temperature (maximum at 423 K) and that carbon contamination was less.

Carburization of Nb_2O_5 in the Presence of NiMo Catalyst

Niobium pentoxyde was mixed with 50 wt% of NiMo catalyst bead shaped This mixture, referred to as $NiMo/Nb_2O_5$, was carburized at atmospheric pressure in a flow of 80 vol% methane in hydrogen. Typically, for 1 g of $NiMo/Nb_2O_5$ the flow rate of carburizing mixture was 85 $cm^3\,min^{-1}$, and the heating rate was 2.5 $K\,min^{-1}$ from 293 to 600 K and then 0.5 $K\,min^{-1}$ up to 1100 K. The carburization process was followed by gas chromatography analysis of gaseous products flowing out of from the reactor. The comparison, displayed in Fig. 4, between the methane consumption recorded during the carburization of a sample of NiMo catalyst alone and the methane consumption of a $NiMo/Nb_2O_5$ mixture (all things being equal unless the Nb_2O_5 weight) shows that the peak at 1070 K corresponds to niobium oxide carburization. When the temperature reached 1100 K, the sample was quenched, passivated, and finally sieved in order to separate the carburized Nb_2O_5 powder from the carburized NiMo beads. The X-ray diffraction pattern of the powder obtained by this sieving, pointed out the presence of a cubic phase alone, very close to δ-NbC. However, the chemical analysis showed large contamination by carbon. The main characteristics of the synthesized carbide are reported on Table 2.

Carburization through NbN_xO_y Intermediate

Niobium oxynitride was first prepared by reaction of niobium pentoxyde with pure ammonia flowing at a molar space velocity of 175 h^{-1}.The temperature of nitridation, linearly raised to 923 K, was maintained for 12 h (45). The reactor was flushed with pure helium for 1 h before introducing the methane–hydrogen mixture, flowing at a molar space velocity ranging from 80 to 120 h^{-1}. The oxynitride previously synthesized was then heated at a rate of 0.5 K or 2.5 $K\,min^{-1}$ either until methane consumption had been obtained and achieved or up to 1123 K, this depending on the heating rate and composition of the carburizing mixture. In the latter case the temperature was maintained until the completion of the reaction. In both cases, as soon as the methane consumption had been achieved, the reactor was rapidly cooled and then flushed with pure helium. Gas chromatography of effluents during carburization showed that the formation of carbon monoxide and nitrogen were simultaneous (Fig. 1,3) and simultaneous with the consumption of methane. The composition of the solid product, determined by chemical analysis, was characteristic of niobium carbonitride but with slight variations depending on

TABLE 1
Physico-chemical Properties of Synthetized Niobium Carbides

Precursor	Synthesis conditions[a] T_f/D_H	Synthesis conditions[a] x_{CH_4}	Observed phases by XRD	Cell parameter, a (Å)	Crystallite size, D_c (Å)	C amount (%wt)	Surface area Sg ($m^2\,g^{-1}$)	Particle size, D_p (Å)
Nb_2O_5	1123 K/33	0.1	NbO_2		1900			
			δ-$NbC_{0.81}$	4.4533 (3)	350			
Nb_2O_5	1123 K/28	0.18	δ-NbC	4.4712 (3)	207	11.9	17	453
Nb_2O_5	1123 K/8	0.18	δ-$NbC_{0.97}$	4.4700 (1)	270	11.6	15	513
1% Ni/Nb_2O_5	1123 K/5	0.1	δ-$NbC_{0.99}$	4.4705 (1)	403	11.7	10.9	704
1% Ni/Nb_2O_5	1123 K/2	0.2	δ-$NbC_{0.99}$	4.4805 (1)	180	13.3	18.3	419
1% Rh/Nb_2O_5	1123 K/5	0.1	δ-$NbC_{0.94}$	4.4677 (1)	157	10.9	16.4	468
$NiMo/Nb_2O_5$	1103 K/0	0.8	δ-$NbC_{0.96}$	4.4692 (1)	120	17.6	50	154

[a] T_f is the final temperature of carburization process in Kelvin; D_h the duration, in hours, of the treatment at T_f; x_{CH_4} the molar fraction of methane. For all these synthesis the molar space velocity is $360\,h^{-1}$ except for the $NiMo/Nb_2O_5$ sample.

the synthesis conditions (Table 2). The X-ray diffraction pattern of the passivated sample showed only the typical pattern of a cubic close-packed structure similar to that of δ-NbC but with a shift in peak locations (Fig. 3). Lattice parameter and specific surface area of niobium carbonitrides are reported in Table 2.

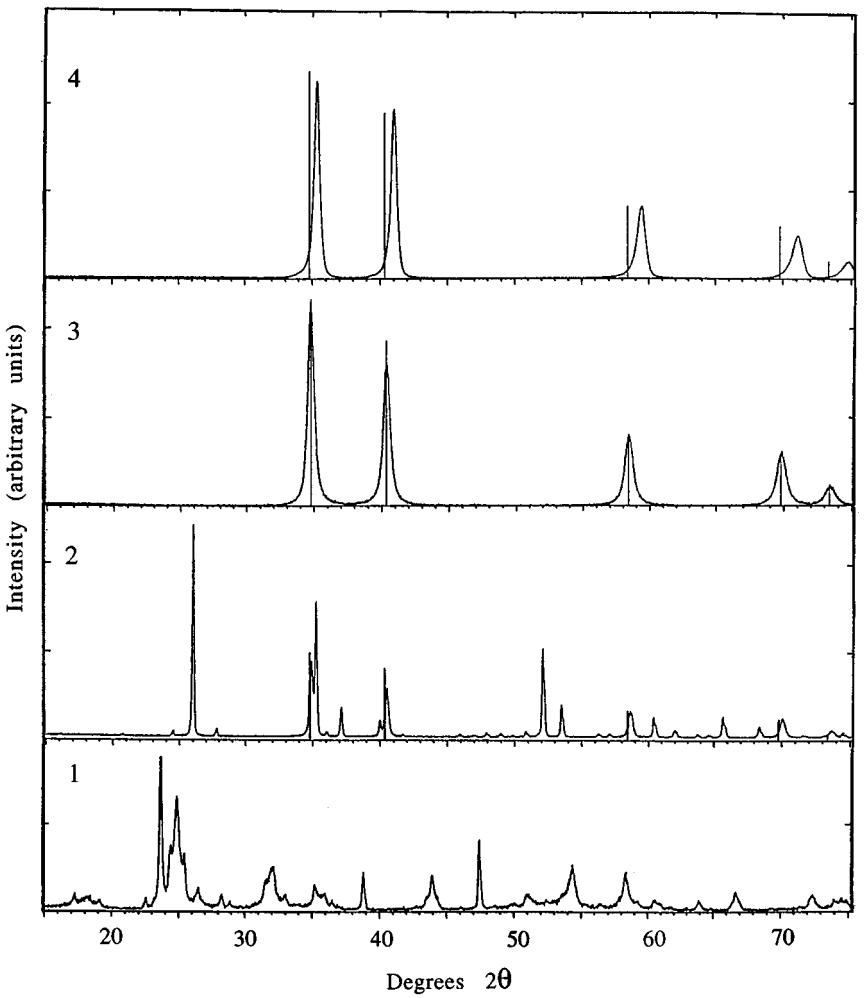

FIG. 3. X-ray diffraction patterns of (1) Nb_2O_5 precursor, (2) partially carburized Nb_2O_5, (3) carburized Nb_2O_5 or Ni/Nb_2O_5, (4) carburized NbN_xO_y. The stick diagram on (2), (3), and (4) represent the location and the relative intensities of δ-NbC X-ray diffraction line.

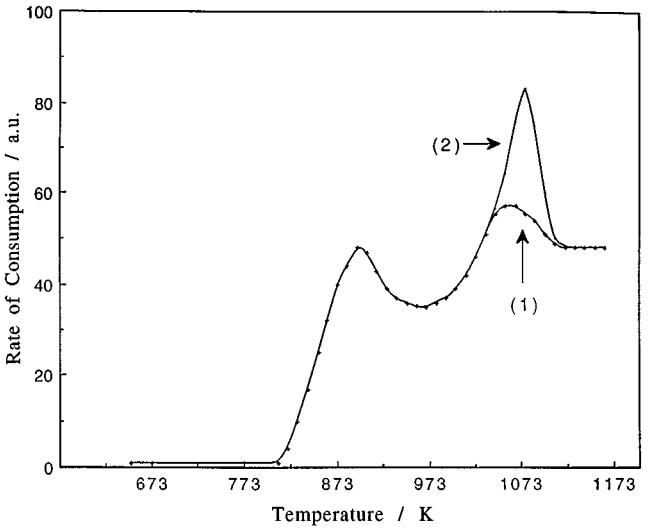

FIG. 4. Comparison between the methane consumption profiles during the carburization of (1) NiMo catalyst alone and (2) $NiMo/Nb_2O_5$ mixture with the same weight of NiMo catalyst and 80% (v/v) CH_4/H_2 mixture. The rate of heating was 0.5 K/min.

DISCUSSION

According to Paris and Clar (30), the carburization of niobium pentoxide by methane–hydrogen mixtures is thermodynamically possible from 1023 K. In pratice, this reaction has been carried out only at higher temperatures, ranging from 1173 to 1373 K (30, 41, 42). The present study confirms this difficulty in carburizing niobium pentoxide, or more exactly NbO_2, which is an intermediate product in carburization, as both the thermogravimetric and the X-ray diffraction analyses show. Moreover, for the commercial precusor that we used (a mixture of two crystallographic varieties M and T) and as already mentioned for niobium pentoxide nitridation (46), the T variety proved more reactive than the M variety and was thus the first to be reduced, giving the shoulder observed at 1053 K on Fig. 1,1 or the second water peak at 978 K in Fig. 1,2.

At 1123 K, the TGA curve (Fig. 2) points out an induction period of several hours before effective NbO_2 carburization begins, wrongly suggesting that the reaction will not take place. Under flowing gas, this induction period varies in length, according to the operating conditions. Using a carburizing mixture of 18 vol% CH_4 in H_2, the induction time is of around 17 h at 1123 K and of 5 h at 1223 K. After this induction period, an acceleratory period was observed. The carburization develops over about 10 h in the first instance and over a little more than 2 h in the second case. We can therefore deduce that the apparent discrepancy between the thermodynamic previsions and the experimental results arise from the presence of a prolonged period of latency in the NbO_2 carburization reaction. This induction period could be linked to the surface state of NbO_2 and its capacity to activate the methane molecule in order to initiate the reduction/carburization process, as shown latter in the presence of a catalyst (Rh, Ni, or $NiMo/Al_2O_3$). This state of surface can depend on the structure and/or the texture of the precursor which can induce the formation of some particular reticular plane, as in Mo_2C synthesis (45) and so explains the difference in reactivity observed between the commercial niobium pentoxide which we used (a mixture of T and M varieties) and that used by Oyama *et al.* (B variety or aerogel) (41, 42).

This induction period is also significantly longer for syntheses under flowing CH4/H2 mixture than for static atmospheric thermobalance syntheses. We consider that the presence of low water pressure promotes the formation of the NbC phase. Later, the presence of this phase activates the decomposition of the methane molecule, giving an autocatalytic aspect to the reaction.

The use of additives (metals or NiMo), likely to catalyze the decomposition of the methane molecule, enabled the suppression of the induction period and increased the carburization speed, as shown in Figs. 1 and 4.

The concentration of methane is another kinetic carburization parameter: the higher the concentration, the quicker the carburization, but, on the other hand, the greater the contamination by free carbon, often called "polymeric" (43)

TABLE 2
Physico-chemical Properties of Synthetized Niobium Carbonitrides

Precursor	Synthesis conditions[a]		Cell parameter, a_0 (Å)	Crystallite size D_c (Å)	C amount (%wt)	N amount (%wt)	Surface area Sg ($m^2\,g^{-1}$)	Particule size D_p (Å)
	T_f	x_{CH_4}						
Nb N_x O_y	1123 K	0.1	4.3971 (2)	192	4.64	10.72	27	284
Nb N_x O_y	1177 K	0.25	4.3781 (12)	145	4.53	11.59	35	219
Nb N_x O_y	1151 K	0.5	4.3556 (6)	133	4.41	11.99	49	156

[a] T_f is the final temperature of carburization process; x_{CH_4} the molar fraction of methane.
The other synthesis conditions are: heating rate = 2.5 K min^{-1}; molar space veloticiy = 120 h^{-1}.

or "pyrolytic" carbon (42) (Table 1). The TGA curves also show that the more active the methane decomposition catalyst, the more rapid is carburization but the greater is the carbon deposition on the final product.

The concentration of methane affects the development of the texture of the end product; indeed the specific surface increases along with methane concentration (Tables 1 and 2). Probably, the free carbon due to the dissociation of methane, which lies at the surface of the carbide crystallites and increases with the concentration of methane, lowers the superficial moblility of atoms, and thus reduces the sintering of these crystallites during the carburization progress.

On the basis of the results of thermogravimetric and chromatographic analyses and X-ray diffraction pattern, the stoichiometries of the two steps of niobium pentoxide transformation can be written as follows:

for the first reduction step,

$$Nb_2O_5 + H_2 \rightarrow 2\,NbO_2 + H_2O \qquad [1]$$

for the reducion/carburization step.

$$NbO_2 + 3CH_4 \rightarrow NbC + 2\,CO + 6\,H_2 \qquad [2]$$

For niobium pentoxide alone, these two steps are markedly distinct. Using a metallic catalyst, the CO release begins at around 893 K, before reduction to NbO_2 has been achieved. In this case, chromatographic evaluation of the amounts of water and of carbon monoxide evolved during the synthesis shows a large deficit in water formation and an excess in carbon monoxide compared to that seen in stoichiometry reactions [1] and [2]. This would suggest that this carbon monoxide arises in part from the thermodynamically possible reaction at these temperatures between H_2O and CH_4.

The value of the cell parameter of the prepared niobium carbides, with or without catalyst, shows that the composition of these carbides is close to the stoichiometric composition NbC (Table 1).

Contamination by superficial free carbon is usually low (below 0.5 wt%) except for carbides prepared in the presence of nickel and in particular of NiMo. The removal of free carbon could not be undertaken using mild oxidation. When niobium carbide is subjected to a mixture of 10 vol% of oxygen in helium and its temperature linearly raised, thermogravimetric analysis and diffraction of X-ray show that niobium carbide oxidizes from 503 K onward in an amorphous compound. This recrystallizes later at a higher temperature in an orthorhombic Nb_2O_5 variety. The free carbon only begins to oxidize at around 773 K.

In fact, the removal of free carbon can be carried out as methane through hydrogen reduction. This occurs at 1073 K, or from 973 K onward in the presence of nickel. The carbidic carbon is also removed but more slowly than free carbon as shown by the chromatographic analysis of methane evolved during the reduction and the XRD analysis of final product. The stoichiometry of carbides depends on the duration and on the final temperature of the reducing treatment.

At a textural level, this treatment did not seriously alter the specific surface of the carbide; at 1223 K the decrease did not exceed 10%. However, the quantity of carbon monoxide irreversibly chemisorbed at room temperature went from zero before reducing treatment, to 68 $\mu mol\,g^{-1}$ (with a surface area of 15 $m^2\,g^{-1}$) after a 1-h reducing treatment at 1223 K. The carbon monoxide uptake by square meter is about two times greater than the one mentioned in recent studies (41, 42).

Niobium oxynitride carburization does not lead to the formation of a monocarbide but to a carbonitride which is probably more stable within the conditions of the synthesis. As for NbO_2, oxygen is removed from the oxynitride structure in the form of carbon monoxide and not as water (Figs. 1–3). Carburization is also accompanied by a partial nitrogen expulsion in molecular form. The carbonitride formula varies according to experimental conditions, around the mean value $NbC_{0.4}N_{0.9}$: the carbon content is much higher and that of nitrogen much lower, when the temperature of synthesis is more raised (Table 2). The diffraction of the X-rays shows that niobium carbonitride has a face-centered cubic structure. As suggested by the chemical composition the cell parameter is closer to that of NbN than to that of NbC. This parameter increases when carbon content increases and when correlatively that of nitrogen diminishes. As in the case of niobium oxynitrides (46) if we take both the composition and the cubic face-centered structure of the compound into consideration, it would appear that the niobium carbonitride must be a nonstoichiometric compound with vacancies in its metallic sublattice.

The specific surface area of carbonitrides can reach 49 $m^2\,g^{-1}$. It is larger when the temperature of synthesis is lower and the methane content is higher. The influence of methane content can be interpreted as in the preceding case for niobium carbide. Just after synthesis, the niobium carbonitride did not chemisorb carbon monoxide, but after a reducing treatment, in flowing hydrogen at 1123 K for 2 h, the carbonitride was found to chemisorb irreversibly CO at room temperature (114 $\mu mol\,g^{-1}$ for a sample with a specific surface area of 35 $m^2\,g^{-1}$).

CONCLUSION

The carburization of the M and T varieties of niobium pentoxide by a hydrogen–methane mixture begins with a reduction by hydrogen from pentoxide to NbO_2; the T variety is reduced before the M variety. No stable intermediate has been evidenced by X-ray diffraction during the reduction of dioxide to niobium monocarbide NbC. The main feature of

this reaction is a long period of induction (5 to 17 h) depending on the synthesis temperature.

Once started, the reduction–carburization process can lead to isothermal development with an acceleratory period up to a reaction extent ranging between 40 and 60%. The carbide composition so synthetized has a composition close to stoichiometric NbC and has a specific surface area of about $15\,m^2\,g^{-1}$. Just after synthesis, the carbide, contaminated by free carbon, does not chemisorb carbon monoxide. In contrast, hydrogen reduction at 1223 K, allowed the irreversible chemisorption of carbon monoxide at room temperature. In the presence of the methane decomposition catalyst, the induction period is suppressed and the reduction and reduction–carburization rates are significantly increased. The specific surface area increases along with the methane content and can reach $50\,m^2\,g^{-1}$, but the free carbon contamination is raised at the same time.

When niobium oxynitride is used as an intermediate, the result is a carbonitride which is nonstoichiometric and probably lacunary in metallic sublattice, of which physicochemical characteristics, composition, and cell parameter differ markedly with the synthesis conditions. This compound can be prepared with a specific surface area of about $50\,m^2\,g^{-1}$. After a reducing treatment in flowing hydrogen at 1123 K, irreversible CO chemisorption at room temperature was observed.

REFERENCES

1. E. K. Storms, B. Calkin, and A. Yencha, *High Temp. Sci.* **1,** 430 (1969).
2. E. Rudy, "Compendium of Phase Diagram Data," AFML-TR-65-2, Part V, 1969.
3. G. Brauer, H. Renner, and J. Wernet, *Z. Anorg. Allg. Chem.* **277,** 249 (1954).
4. R. Lesser and G. Brauer, *Z. Metallk.* **50,** 8 (1959).
5. E. K. Storms and N. H. Krikorian, *J. Phys. Chem.* **64,** 1471 (1960).
6. R. P. Elliot, *Trans. Am. Soc. Metals* **53,** 13 (1961).
7. S. I. Alyamovskii, G. P. Shveikin, P. V. Gel'd, and N. M. Volkova, *Kh. Neorg. Khim.* **12,** 579 (1967).
8. N. Terao, *J. Appl. Phys.* **3,** 104 (1964).
9. K. Yvon, H. Nowotny, and R. Kieffer, *Monatsh. Chem.* **98,** 34 (1967).
10. E. Rudy and C. E. Brukl, *J. Am. Ceram. Soc.* **50,** 265 (1967).
11. B. V. Khaenko and O. A. Gnitetskii, *Kristallografiya* **38,** 55 (1993).
12. E. K Storms and N. H. Krikorian, *J. Phys. Chem.* **63,** 1747 (1959).
13. E. K Storms, N. H. Krikorian, and C. P. Kempter, *Anal. Chem.* **32,** 1722 (1960).
14. C. P. Kempter, E. K. Storms, and R. J. Fries, *J. Chem. Phys.* **33,** 1873 (1960).
15. A. I. Gusev and A. A. Rempel, *Phys. Status. Solidi* A **163,** 273 (1997).
16. A. A. Rempel, A. I. Gusev, V. G. Zubkov, and G. P. Shveikin, *Dokl. Akad. Nauk SSSR* **275,** 883 (1984).
17. A. A. Rempel, M. Yu. Belyaev, L. B. Dubrovskaya, and G. P. Shveikin, *Zh. Neorg. Khim.* **29,** 2451 (1984).
18. A. I. Gusev and A. A. Rempel, *Fiz. Tverd. Tela* (*Leningrad*) **26,** 3622 (1984).
19. A. A. Rempel and A. I. Gusev, *Kristallografiya* **30,** 1112 (1985).
20. A. A. Rempel, A. I. Gusev, and M. Yu. Belyaev, *J. Phys. C* **20,** 5655 (1987).
21. B. V. Khaenko and O. P. Sivak, *Kristallografiya* **35,** 1110 (1990).
22. C. Agte and K. Moers, *Z. Anorg. Allg. Chem.* **198,** 233 (1931).
23. V. Ya. Naumenko, *Poroshk. Metall.* **10,** 20 (1970).
24. Z. A. Munir, *Ceram. Bull.* **67,** 342 (1988).
25. Y. Zhang and G. C. Stangle, *J. Mater. Res.* **10,** 962 (1995).
26. G. P. Shveikin, *Trudy Inst. Khim. Akad. Nauk SSSR, Ural Filial.* **2,** 57 (1958).
27. Masumoto Osamu and Saito Michio, *High Temp. Sci.* **6,** 135 (1974).
28. G. K. Moiseev, S. K. Popov, L. A. Ovchinnikova, and N. A. Vatolin, *Izv. Akad. Nauk SSS, Neorg. Mater.* **19,** 72 (1993).
29. Shimada Shiro, Koyama Tadashi, Kodaira Kohei, and Mastushita Toru, *J. Mater. Sci.* **18,** 1291 (1983).
30. R. A. Paris and E. Clar, *Chim. Ind. Genie Chim.* **102,** 57 (1969).
31. Yu. A. Pavlov, V. P. Polyakov, V. V. Gal, K. A. Nikitin and T. M. Skachkova, *Izv. Vyssh. Ucheb. Zaved. Chem. Met.* **14,** 5 (1971).
32. S. T. Oyama, J. C. Schlatter, J. E. Metcalfe III, and J. M. Lambert, Jr., *Ind. Eng. Chem. Res.* **27,** 1639 (1988).
33. C. Agte and K. Moers, *Z. Anorg. Allg. Chem.* **198,** 243 (1931).
34. I. V. Petrusevich, L. A. Nisel'son, Yu. A. Chernukhin, and F. N. Kozlov, *Izv. Akad. Nauk SSSR. Neorg. Mater.* **6,** 2200 (1970).
35. V. F. Funke, A. I. Tyutyunnikov, V. S. Makee, A. N. Pilyugin, and V. A. Shevchenko, *Poroshk. Metall.* **6,** 44 (1976).
36. R. M. Powel, W. J. Skocpol, and M. Tinkham, *J. Appl. Phys.* **48,** 788 (1977).
37. N. V. Alekseev, Yu. B. Blagoveshchenskii, G. N. Zviadadze, and I. K. Tagirov, *Poroshk. Metall.* **8,** 1 (1980).
38. Yu. V. Blagoveshchenskii, G. N. Eviadadze, and I. K. Tagirov, *Fiz. Khim. Obgab. Mater.* **6,** 32 (1982).
39. P. Matteazzi and G. Le Caer, *J. Am. Ceram. Soc.* **74,** 1382 (1991).
40. Liu Lin, Li Bing, Ding Xing-Zhao, Ma Xue-Ming, Qi Zhen-Zhong, and Dong Yuan-Da, *Chin. Sci. Bull.* **39,** 1166 (1994).
41. V. L. S. Teixeira da Silva, E. I. Ko, M. Schmal, and S. T. Oyama, *Chem. Mater.* **7,** 179 (1995).
42. V. L. S. Teixeira da Silva, M. Schmal, and S. T. Oyama, *J. Solid State Chem.* **123,** 168 (1996).
43. J. S. Lee, S. T. Oyama, and M. Boudart, *J. Catal.* **106,** 125 (1987).
44. L. Volpe and M. Boudart, *J. Solid State Chem.* **59,** 348 (1985).
45. J. S. Lee, L. Volpe, F. H. Riberio, and M. Boudart, *J. Catal.* **112,** 44 (1988).
46. H. S. Kim, C. H. Shin, G. Bugli, M. Bureau-Tardy, and G. Djéga-Mariadassou, *Appl. Catal. A* **119,** 223 (1994).
47. S. Brunauer, P. H. Emmet, and E. Teller, *J. Amer. Chem. Soc.* **60,** 309 (1938).
48. D. E. Williams, LCR-2, "A Fortran Lattice Constant Refinement Programm," USAEC Reports IS-1052, 1964.
49. J. I. Langford and A. J. C. Wilson, *J. Appl. Crystallogr.* **11,** 102 (1978).